AERODYNAMIC DERIVATIVES FOR OSCILLATING THREE-DIMENSIONAL WINGS IN TRANSONIC FLOW

By MÅRTEN T. LANDAHL

The Aeronautical Research Institute of Sweden

Summary—Some linearized solutions for generalized aerodynamic forces on oscillating three-dimensional wings in transonic flow are presented. Linearized theory is valid whenever the reduced frequency of oscillation is not too low.

For the rectangular wing the solution is given as an infinite series in which the solution for the wing of infinite span constitutes the initial term. This series is shown to be convergent for all non-zero aspect ratios and converges very rapidly even for comparatively low aspect ratios. Three terms are found to be sufficient in most practical cases. The numerical calculations have been programmed on a high-speed electronic computer and some results for a wing–aileron combination are given. The results show that three-dimensional effects are very important and, in particular, increase the damping of the rotational degree of freedom of the aileron.

Solutions for other planforms are also considered briefly. For triangular wings a special transformation is given which relates the solution to that for a rectangular wing.

1. INTRODUCTION

THEORY and experiments indicate that the danger of an airplane or missile encountering flutter or other instabilities of aerodynamic origin usually is greatest at transonic speeds. That strong unsteady-flow effects should exist in this speed range can readily be explained when remembering that in a transonic flow disturbances travel forward at about the same speed as the object causing them. Thus even a slow unsteady motion may set up large phase differences between different parts of the flow field and unstabilizing phase relations between motion and aerodynamic force may therefore easily be created.

The efforts to make accurate flutter predictions are seriously hampered by the present scarcity of adequate tables for aerodynamic forces on oscillating three-dimensional wings. For high supersonic Mach numbers or for large-aspect-ratio wings in subsonic flow the use of the strip (two-dimensional) theory may be justified. At transonic speeds, however, cross-flow effects are always very large (cf. the transonic area rule) so that the strip theory would lead to large errors in the computed flutter speed.

In the present paper the solution is given for rectangular wings of arbitrary aspect ratio and a transformation is also presented which relates the solution for a delta wing to that of a rectangular wing. The theory is based on the linearized equations of motion which are applicable also for transonic flow, provided the reduced frequency is not too low.

2. SYMBOLS

A	aspect ratio of wing or control surface
b	reference chord
$C(x) - iS(x) = \int_0^x \frac{e^{-iu}}{\sqrt{2\pi u}}\,du$	Fresnel integrals
C_p	pressure coefficient
$f(x, y)$	mode shape function
$h_0(x, y)$	solving kernel given by Eq. (A8)
$k = \frac{\omega b}{U}$	reduced frequency
$K=(2ks+k^2)^{\frac{1}{2}}$	
$L_{ij} = \lvert L_{ij}\rvert\, e^{i\theta_{ij}}$	generalized aerodynamic force coefficients defined by Eq. (27)
$l_{ij} = \lvert l_{ij}\rvert\, e^{i\phi_{ij}}$	sectional aerodynamic force coefficients defined by Eq. (29)
M	free-stream Mach number
M_L	local Mach number
q	dynamic pressure
r, θ, ρ / $\bar{r}, \bar{\theta}, \bar{\rho}$	polar co-ordinate systems defined in Fig. 3
s	Fourier transform variable
S	reference area (wing or control surface area)
t	time
U	free-stream velocity
$w(x, y)$	normal velocity of wing
$W(y)$	Fourier transform of $w(x, y)$
x, y, z	Cartesian co-ordinate system given in Fig. 1
X, Y, Z	transformed co-ordinate system defined by Eq. (47)
δ	non-dimensional amplitude of oscillation
ϵ	thickness ratio
σ	semi-span-to-chord ratio
Φ	Fourier transform of φ
ϕ	$= Re\{\varphi e^{i\omega t}\}$, dimensionless perturbation velocity potential, $\varphi = \sum_0^\infty \varphi^{(n)}$

$\psi^{(n)}$, $\bar{\psi}^{(n)}$	side-edge correction potential to the nth order for the right and left hand side edge, respectively
$\Psi^{(n)}$, $\bar{\Psi}^{(n)}$	Fourier transforms of $\psi^{(n)}$, $\bar{\psi}^{(n)}$
ξ, η	dummy variables
Ω	transformed potential function for the delta wing, Eq. (48)
ω	angular frequency of oscillation

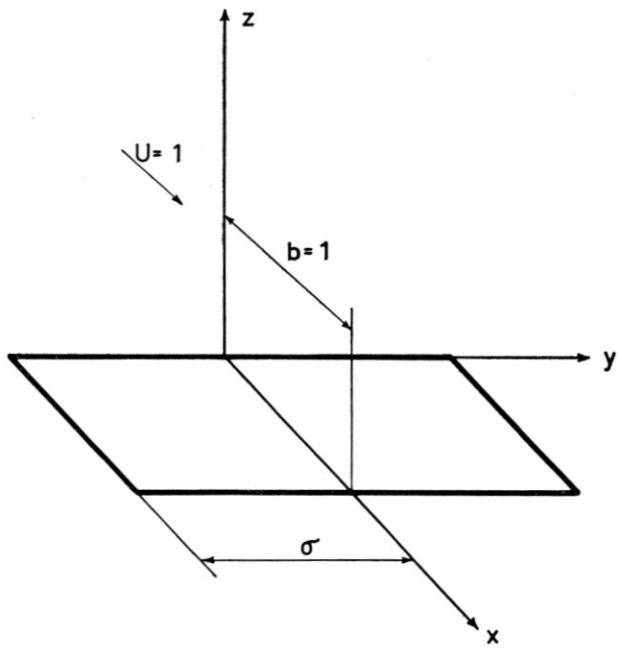

FIG. 1. Co-ordinate system.

3. LINEARIZATION OF THE EQUATIONS OF MOTION

Typical of transonic flow is the non-linear accumulation of flow disturbances moving very slowly with respect to the body causing them. This will in general prohibit the use of linear theory for steady flow. If the flow oscillates rapidly, however, the disturbances will not have time to accumulate and linear theory will be applicable with similar accuracy as in sub- or supersonic flow. Quantitative conditions for linearization to be possible in two-dimensional flow were first given by Lin, Reissner, and Tsien[1] and their analysis has later been extended to three-dimensional flow[2, 3, 4]. The results show that linearization is possible provided the reduced frequency of oscillation $k = (\omega b)/U$ is so high that the following requirement is fulfilled everywhere in the flow

$$k \gg |1-M_L| \tag{1}$$

where M_L is the local Mach number. In two-dimensional flow $1 - M_L = 0(\epsilon^{\frac{2}{3}})$ (ϵ = thickness-to-chord ratio) and for low-aspect-ratio wings $1 - M_L = 0\,(\epsilon\,\sigma \ln \sigma\,\epsilon^{\frac{1}{2}})$ (σ = semispan-to-chord ratio) so that linearization should work down to lower reduced frequences in the low-aspect-ratio than in the two-dimensional case.

The condition (1) will make the wave lengths of the disturbances moving slowly with respect to the body so small that neighbouring waves will have time to interact and damp out before having travelled but a small distance compared to the characteristic length of the body. The proper linearized differential equation for the perturbation velocity potential $\phi = Re[\varphi e^{i\omega t}]$ in non-dimensional form then reads[4]

$$\varphi_{yy} + \varphi_{zz} - 2ikM^2\varphi_x + k^2M^2\varphi = 0 \tag{2}$$

The non-dimensional co-ordinates are chosen so that $b = U = 1$. This then requires the frequency of oscillation, ω, to be equal to the reduced frequency k.

4. GENERAL SOLUTION FOR A RECTANGULAR WING

The Mach number can be eliminated very simply from Eq. (2) by the transformation $\bar{y} = My$; $\bar{z} = Mz$, so we may in the following set $M = 1$.

Let the amplitude distribution of the rigidly or flexibly oscillating wing be given by $z = \delta f(x,y)$ where δ is the non-dimensional amplitude and $f(x,y)$ is the mode shape function. Then the boundary condition on the wing reads

$$\varphi_z(x,y,0) = w(x,y) = \delta(f_x + ikf) \tag{3}$$

for $0 \leqslant x \leqslant 1$; $|y| \leqslant \sigma$

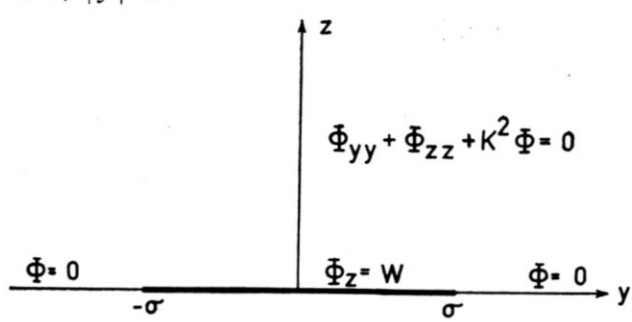

FIG. 2. Boundary value problem after Fourier transformation.

Outside the wing the pressure difference across $z = 0$ should be zero. Hence

$$\varphi(x,y,0) = 0 \text{ for } |y| \geqslant \sigma \tag{4}$$

Together with the condition of non-reflection at infinity (Sommerfeld) and that φ should vanish upstream of the wing, this formulates our boundary

value problem. For its solution we will employ Fourier transforms. Transformed variables will be denoted by capital letters so that, for example,

$$\Phi = \frac{1}{\sqrt{2\pi}} \int_{-\infty}^{\infty} \varphi e^{-isx} \mathrm{d}x = \mathcal{F}\{\varphi\} \tag{5}$$

The boundary value problem then takes the following form (see Fig. 2)

$$\Phi_{yy} + \Phi_{zz} + K^2 \Phi = 0 \tag{6}$$

$$\Phi_z(y,0) = W \qquad \text{for } |y| \leqslant \sigma \tag{7}$$

$$\Phi(y,0) = 0 \qquad \text{for } |y| \geqslant \sigma \tag{8}$$

where

$$K = (2ks + k^2)^{\frac{1}{2}} \tag{9}$$

We will select that branch of K for which $\mathrm{Im}(K) < 0$ and a suitable cut is therefore introduced in the complex s-plane.

Eqs. (6)–(8) plus the condition that Φ should vanish at infinity define the classical problem of two-dimensional diffraction around a finite strip. For its solution two different methods are available in the literature. In the first one elliptical co-ordinates are introduced. Then the problem can be solved by separation of variables in terms of Mathieu functions. This method was used by Miles[7] when treating the oscillating low-aspect-ratio rectangular wing in supersonic flow. Due to the complexity of the Mathieu functions, however, this method is not suited for the present problem since the inversion of the Fourier transforms will lead to excessive difficulties.

The second method, which will be used here, is the one originally given by Schwarzschild[8]. In this a first order solution is obtained by disregarding the boundary condition, Eq. (8), that the potential should be zero on the y-axis outside the wing strip. Then a solution is added which cancels the first order solution on the y-axis for $y \geqslant \sigma$ but leaves the normal derivative unchanged for $y < \sigma$. This is repeated for the other edge and the process is continued until the desired accuracy is attained (see Fig. 4). This method was used by Gunn[9] to calculate the lifting pressures on a low-aspect-ratio rectangular wing at incidence in supersonic flow.

The solution for $z \geqslant 0$ of the first order problem, $\Phi^{(0)}$, is easily found by standard methods to be

$$\Phi^{(0)} = \frac{i}{2} \int_{-\infty}^{\infty} H_0^{(2)}(KR)\, W(\eta)\, \mathrm{d}\eta \tag{10}$$

where

$$R = \sqrt{(y-\eta)^2 + z^2}$$

Here $W(y)$ should be suitably continued for $|y| > \sigma$. If W is independent of y it is convenient to let it remain constant to $|y| = \infty$. Then the integration in Eq. (10) may be carried out with the result that

$$\Phi^{(0)} = \frac{iW(s)}{K} e^{-iKz} \tag{11}$$

Upon inversion this leads to the ordinary strip theory solution, as given e.g. in Ref. 10.

Setting $W(y) = 0$ for $y > \sigma$ leads to the Kirchhoff approximation which will be discussed in Section 6.

At this stage it is convenient to introduce two sets of polar co-ordinates r, θ and $\bar{r}, \bar{\theta}$ with origins at the right and left edges, respectively (see Fig. 3). On the wing $\theta = \bar{\theta} = \pi$. The distances from a point on the y-axis outside the wing strip to the nearest edge are denoted by ρ and $\bar{\rho}$, respectively (these are used as integration variables).

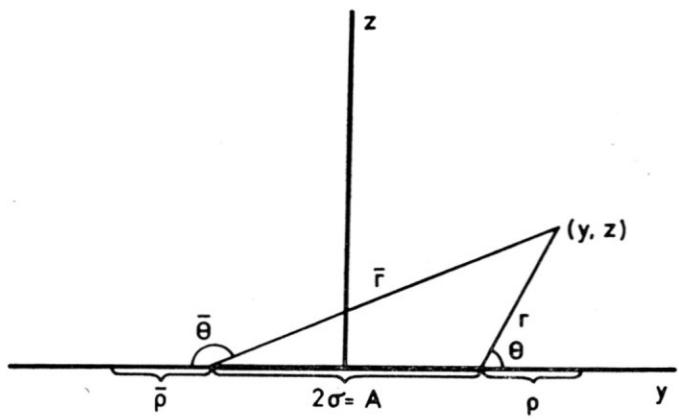

FIG. 3. Auxiliary co-ordinate system.

We will now seek a solution $\Psi^{(1)}(r,\theta)$ to the wave equation (6) with $\Psi^{(1)} = -\Phi^{(0)}(y) = -\Phi^{(0)}(\sigma + \rho)$ on the y-axis for $y \geqslant \sigma$ and with $\Psi_z^{(1)} = -(1/r)\Psi_\theta^{(1)} = 0$ for $y < \sigma$. The solution on the wing strip, i.e. for $\theta = \pi$, to this boundary value problem was found by Schwarzschild[8] to be

$$\Psi^{(1)}(r) = -\frac{1}{\pi}\int_0^\infty \sqrt{\frac{r}{\rho}}\,\frac{e^{-iK(r+\rho)}}{r+\rho}\,\Phi^{(0)}(\rho + \sigma)\,d\rho \tag{12}$$

The corresponding solution $\bar{\Psi}^{(1)}$ that cancels $\Phi^{(0)}(y)$ on the negative y-axis for $y \leqslant -\sigma$ reads

$$\bar{\Psi}^{(1)}(\bar{r}) = -\frac{1}{\pi}\int_0^\infty \sqrt{\frac{\bar{r}}{\bar{\rho}}}\,\frac{e^{-iK(\bar{r}+\bar{\rho})}}{\bar{r}+\bar{\rho}}\,\Phi^{(0)}(-\sigma - \bar{\rho})\,d\bar{\rho} \tag{13}$$

Hence a second order solution $\Phi = \Phi^{(0)} + \Phi^{(1)}$ is obtained, where

$$\Phi^{(1)} = \Psi^{(1)} + \bar{\Psi}^{(1)} \tag{14}$$

However, Φ will still not be zero for $|y| \geqslant \sigma$ since $\Psi^{(1)}$ does not vanish for $r > A$, except if $KA \to \infty$, and vice versa for $\bar{\Psi}^{(1)}$. Therefore a solution $\Phi^{(2)} = \Psi^{(2)} + \bar{\Psi}^{(2)}$ is added, where

$$\Psi^{(2)} = -\frac{1}{\pi}\int_0^\infty \sqrt{\frac{r}{\rho}}\,\frac{e^{-iK(r+\rho)}}{r+\rho}\,\bar{\Psi}^{(1)}(\rho + A)\,\mathrm{d}\rho \tag{15}$$

and $\bar{\Psi}^{(2)}$ is given by an analogous formula.

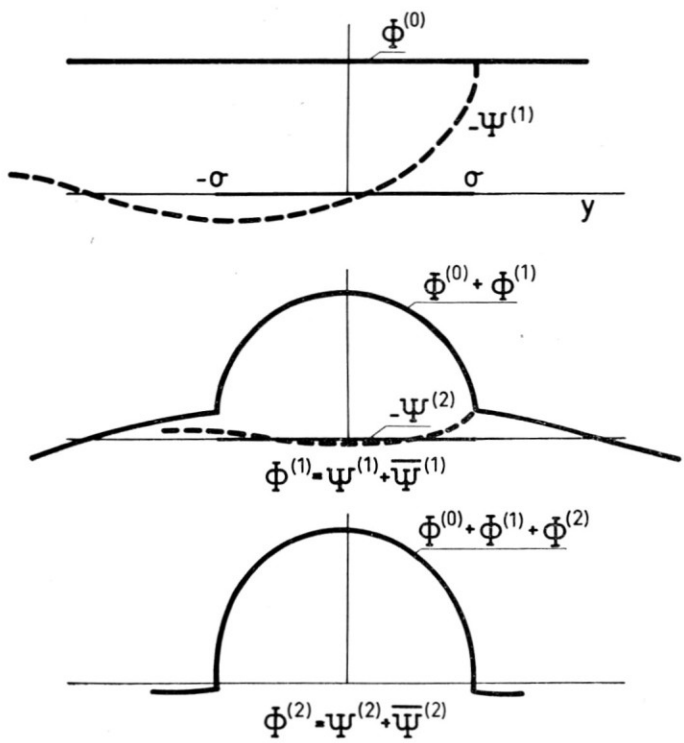

FIG. 4. Principle of solution.

The process which is depicted schematically in Fig. 4 may be continued *ad infinitum*. Schwarzschild showed that, in the case of W independent of y, the infinite series thus obtained converges for all non-zero values of KA. This proof may be extended to cases where $W(y)$ is not independent of y and K a complex number. Thus the following general solution on the wing is found

$$\Phi = \sum_0^\infty \Phi^{(n)} \tag{16}$$

where

$$\left.\begin{aligned} \Phi^{(n)} &= \Psi^{(n)}(r) + \bar{\Psi}^{(n)}(\bar{r}) \qquad (17)\\ \Psi^{(n)} &= -\frac{1}{\pi}\int_0^\infty \sqrt{\frac{r}{\rho}}\,\frac{e^{-iK(r+\rho)}}{r+\rho}\,\bar{\Psi}^{(n-1)}(\rho + A)\,\mathrm{d}\rho \qquad (18)\\ \bar{\Psi}^{(n)} &= -\frac{1}{\pi}\int_0^\infty \sqrt{\frac{\bar{r}}{\bar{\rho}}}\,\frac{e^{-iK(\bar{r}+\bar{\rho})}}{\bar{r}+\bar{\rho}}\,\Psi^{(n-1)}(\bar{\rho} + A)\,\mathrm{d}\bar{\rho} \qquad (19) \end{aligned}\right\} n > 1$$

and $\Phi^{(0)}$, $\Psi^{(1)}$ and $\bar{\Psi}^{(1)}$ are given by Eqs. (10), (12) and (13), respectively.

The inversion to the physical plane is readily carried out by aid of the Faltung theorem for Fourier integrals and the following inversion formulas, valid for $x > 0$,

$$\mathscr{F}^{-1}\left\{H_0^{(2)}(Ka)\right\} = \sqrt{\frac{2}{\pi}}\,\frac{i}{x}\,e^{-i\frac{k}{2}\left[x+\frac{a^2}{x}\right]} \tag{20}$$

$$\mathscr{F}^{-1}\left\{e^{-iKa}\right\} = e^{\frac{\pi i}{4}}\,\frac{a\sqrt{k}}{x^{3/2}}\,e^{-i\frac{k}{2}\left[x+\frac{a^2}{x}\right]} \tag{21}$$

(For $x < 0$ the inverse transforms are zero)

Thus the final result reads

$$\varphi = \sum_0^\infty \varphi^{(n)} \tag{22}$$

$$\varphi^{(n)} = \psi^{(n)} + \bar{\psi}^{(n)} \tag{23}$$

where

$$\varphi^{(0)}(x, y, +0) = -\frac{1}{2\pi}\int_{-\infty}^{\infty} \mathrm{d}\eta \int_0^x \frac{\mathrm{d}\xi}{x-\xi}\,e^{-i\frac{k}{2}\left[x-\xi+\frac{(y-\eta)^2}{x-\xi}\right]} w(\xi, \eta) \tag{24}$$

$$\psi^{(n)}(x, r) = -e^{\frac{\pi i}{4}}\,\frac{\sqrt{2k}}{2\pi^{3/2}}\int_0^\infty \sqrt{\frac{r}{\rho}}\,\mathrm{d}\rho \int_0^x \frac{\mathrm{d}\xi}{(x-\xi)^{3/2}}\,e^{-i\frac{k}{2}\left[x-\xi+\frac{(r+\rho)^2}{x-\xi}\right]} \times \bar{\psi}^{(n-1)}(\xi, A+\rho) \tag{25}$$

$$\bar{\psi}^{(n)}(x, \bar{r}) = -e^{\frac{\pi i}{4}}\,\frac{\sqrt{2k}}{2\pi^{3/2}}\int_0^\infty \sqrt{\frac{\bar{r}}{\bar{\rho}}}\,\mathrm{d}\bar{\rho} \int_0^x \frac{\mathrm{d}\xi}{(x-\xi)^{3/2}}\,e^{-i\frac{k}{2}\left[x-\xi+\frac{(\bar{r}+\bar{\rho})^2}{x-\xi}\right]} \times \psi^{(n-1)}(\xi, A+\bar{\rho}) \tag{26}$$

For $n = 1$ $\psi^{(0)}$ and $\bar{\psi}^{(0)}$ in Eqs. (25) and (26) are to be replaced by $\varphi^{(0)}$.

5. GENERALIZED AERODYNAMIC FORCES

The generalized aerodynamic forces are defined as follows

$$L_{ij} = L'_{ij} + iL''_{ij} = |L_{ij}|e^{i\theta_{ij}} = (qSe^{i\omega t}\delta_i)^{-1}\int_{-\infty}^{\infty}\int_{-\infty}^{\infty}\Delta P_i f_j \, dx \, dy \tag{27}$$

where $\Delta P_i(x, y)$ is the lifting pressure difference due to the mode f_i. In linear approximation this is given by

$$\Delta C_p = 4e^{i\omega t}(\varphi_x + ik\varphi)_{z=+0} \tag{28}$$

For flutter purposes it is sometimes convenient to define sectional coefficients $l_{ij} = l'_{ij} + il''_{ij} = |l_{ij}|e^{i\theta_{ij}}$ by setting

$$L_{ij} = \int_{-\infty}^{\infty}\frac{b}{S}l_{ij} \, dy \tag{29}$$

where $b(y)$ here denotes the local chord.

In particular we will consider rigid body translational and pitching oscillations about $x = 0$ defined by

$$f_1 = 1 \tag{30}$$

$$f_2 = x \tag{31}$$

Thus L_{11} represents total lift due to translation, L_{22} moment due pitch about $x = 0$, etc.

6. CALCULATION FOR A RECTANGULAR WING OSCILLATING IN RIGID TRANSLATION AND PITCH

Although the formulas Eqs. (22)–(26) given in the physical plane may be directly applied it is actually more convenient to carry out the calculation in the transformed plane before inversion.

We will take the first order solution to be the strip theory one. Thus from Eq. (11), for $z = +0$,

$$\Phi^{(0)} = \frac{i}{K}W \tag{32}$$

which upon inversion gives[10]

$$\varphi^{(0)} = -e^{\frac{-\pi i}{4}}\int_0^x \frac{e^{-i\frac{k}{2}(x-\xi)}}{\sqrt{2\pi k(x-\xi)}}w(\xi) \, d\xi \tag{33}$$

For the calculation of $\Psi^{(1)}$ we need the following integral

$$\frac{1}{\pi}\int_0^\infty \sqrt{\frac{r}{\rho}}\,\frac{e^{-iK(r+\rho)}}{r+\rho}\,d\rho = -(1+i)\left[F(Kr) - \frac{1}{2} + \frac{i}{2}\right] \tag{34}$$

where

$$F(x) = \int_0^x \frac{e^{-iu}}{\sqrt{2\pi u}}\,du = C(x) - iS(x) \tag{35}$$

(This integral formula may be proved by differentiating the left-hand side of Eq. (34) with respect to K.)

Thus

$$\Psi^{(1)}(r) = \bar{\Psi}^{(1)}(r) = \frac{i-1}{K}\left[F(Kr) - \frac{1}{2} + \frac{i}{2}\right]W \tag{36}$$

The inversion to the physical plane may be written

$$\psi^{(1)}(x, r, \pi) = \int_0^x h_0(x-\xi, r)\, e^{-i\frac{k}{2}(x-\xi)}\, w(\xi)\, d\xi \tag{37}$$

where h_0 is given in the Appendix. The numerical calculation of the aerodynamic coefficients associated with $\varphi^{(0)}$ and $\psi^{(1)}$ is described in Ref. 5.

Eq. (37) gives the side-edge effect calculated for each edge separately as if the wing were semi-infinite[5]. The two-term solution $\varphi = \varphi^{(0)} + \varphi^{(1)}$ would hence be expected to represent the true solution with good accuracy when the span is large in terms of the wave length, i.e. when $A\sqrt{k}$ is large. Therefore, in order to simplify the analysis, only such large values of $A\sqrt{k}$ will be considered so that the main portion of the side-edge effect is taken care of by $\varphi^{(1)}$ and the higher order terms only give small additional corrections. Actually, as will be evident from the numerical results below, this does not seriously limit the analysis from a practical point of view.

In calculating $\Psi^{(2)}$ the asymptotic value of $\bar{\Psi}^{(1)}$ for large values of $K\bar{r}$ is therefore substituted in Eq. (18). From Eqs. (36) and (35) we find that

$$\bar{\Psi}^{(1)}(\pi, \bar{r}) = \frac{1-i}{\sqrt{K}}\int_{\bar{r}}^\infty \frac{e^{-iKu}}{\sqrt{2\pi u}}\,du \approx -\frac{1+i}{K^{3/2}}\,\frac{e^{-iK\bar{r}}}{\sqrt{2\pi\bar{r}}} \tag{38}$$

Thus

$$e^{-iK(r+\rho)}\bar{\Psi}^{(1)}(\rho + A) \approx \sqrt{\frac{2\rho + A + r}{\rho + A}}\,\bar{\Psi}^{(1)}(2\rho + r + A) \tag{39}$$

or, upon substituting in Eq. (18),

$$\Psi^{(2)}(r, \pi) = -\frac{1}{\pi}\int_0^\infty \sqrt{\frac{r(2\rho + A + r)}{\rho(\rho + A)}}\,\frac{\bar{\Psi}^{(1)}(2\rho + A + r)}{r + \rho}\,d\rho \tag{40}$$

Since s only enters in $\bar{\Psi}^{(1)}$ the inversion becomes simply as follows

$$\psi^{(2)}(x, r, \pi) = -\frac{1}{\pi}\int_0^\infty \sqrt{\frac{r(2\rho + A + r)}{\rho(\rho + A)}}\,\frac{\bar{\Psi}^{(1)}(x, 2\rho + r + A)}{r + \rho}\,\mathrm{d}\rho \quad (41)$$

This integral would have to be evaluated numerically. Any number of differentiations and integrations of each side of Eq. (41) with respect to x can be made without changing the kernel of the integral so that this formula is valid for the associated aerodynamic coefficients as well.

By introducing Eqs. (33), (37) and (41) into the formulas of Section 5 the aerodynamic coefficients may then be evaluated. The numerical calculations for the present paper were performed on the Swedish electronic computer BESK. Results for an $A = 2$ wing are given in Figs. 5–7. This is an aspect ratio typical for wings of practical interest and is so low that it should give a serious test on the convergence of the series (22).

In Fig. 5 sectional lift due to pitching about $x = 0$, i.e. $l_{21} = |l_{21}|e^{i\theta_{21}}$, is shown for $k = 0{\cdot}3$. It is seen that the contribution from the third term is fairly small even at this low frequency. Hence the two-term solution, for which the side-edge effect from each edge is calculated as if

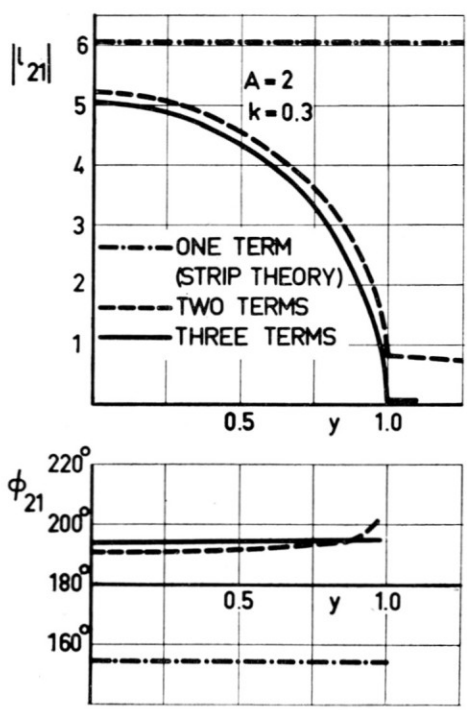

FIG. 5. Spanwise distribution of lift due to pitch about $x = 0$ on a rectangular wing at $M = 1$. $l_{21} = |l_{21}|e^{i\phi_{21}}$.

the wing were semi-infinite[5] gives a fairly good approximation even at rather low values of k and A. As noted earlier in Ref. 11, the strip theory, on the contrary, is very poor, as would be expected.

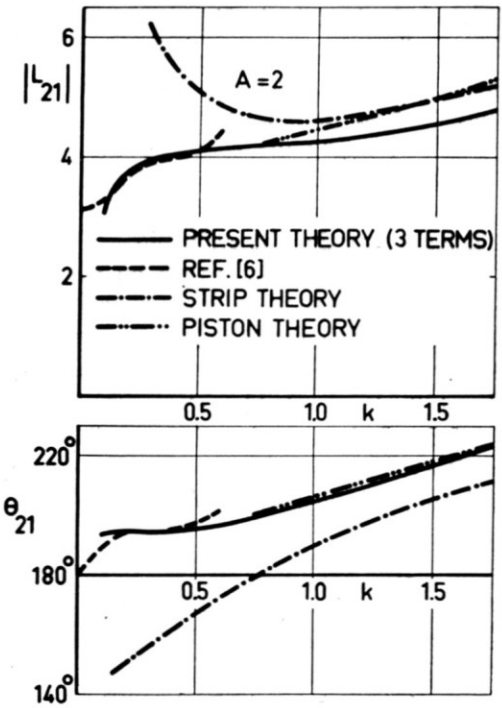

FIG. 6. Coefficient of total lift due to pitch for a rectangular wing at $M = 1$. $L_{21} = |L_{21}|e^{i\theta_{21}}$.

In Fig. 6 the total coefficient of lift due to pitch, L_{21}, is plotted as function of k, and the present three-term solution compared with other approximate theories. At the lower values of k very good agreement is obtained with a recent theory[6] valid for low values of $A\sqrt{k}$. Only below $k = 0{\cdot}1$ the present three-term solution starts to deviate considerably from the low-frequency solution. As discussed in Section 3, however, linearized theory ceases to be valid for very low values of k so that the three-term solution probably covers with sufficient accuracy the whole range of reduced frequencies for which linearization is possible.

For large values of k one would expect strip theory to become progressively more accurate. However, even at the highest frequency shown in Fig. 6 ($k = 1{\cdot}75$) the agreement with the present theory is not particularly good. Actually, the piston theory[3] which is the high-frequency limit of any theory for compressible flow, happens to give better results over the whole frequency range for such a low-aspect ratio wing. In particular it does not show the spurious 45° phase lag at $k = 0$ exhibited by the strip theory.

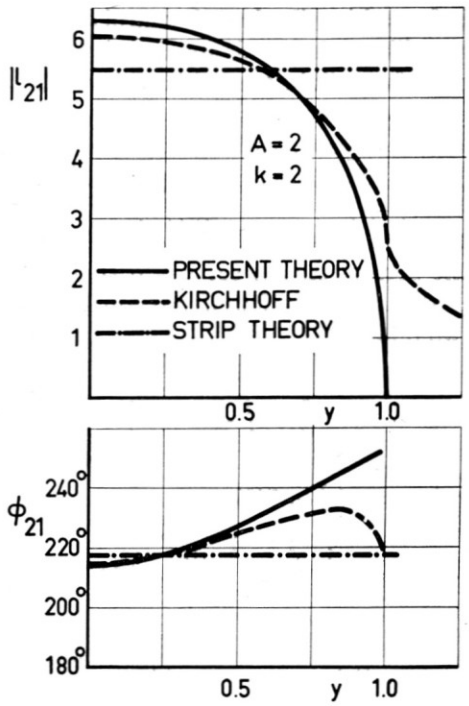

FIG. 7. Comparison of different high-frequency theories for the spanwise distribution of lift due to pitch on a rectangular wing at $M=1$.

To conclude this section a comparison is given between the Kirchhoff approximation and the present solution. The idea behind this approximation is that for a wave length that is small compared to the span one could neglect the flow spill-over around the edges and hence compute φ from Eq. (10) by setting $w(x, y) = 0$ for $|y| > \sigma$. Therefore the fairly high reduced frequency of $k = 2$ is chosen in Fig. 7 where l_{21} is plotted for the $A = 2$ wing. As would be expected the error of the Kirchhoff approximation is largest near the edges where it is about 50 % of the strip-theory value in vector magnitude and 30° in phase angle. Further inboard it is somewhat better. However, it can be shown from the present results that the side edge effect given by Kirchhoff's solution is only $2^{-\frac{1}{2}}$ of the correct value (which is given by $\varphi^{(1)}$) as k becomes large so that this approximation is the correct limiting solution for $k \to \infty$ only in so far as it then leads to the strip theory. Hence its value in the present connexion is doubtful, particularly since it is not simpler to evaluate than the present two-term solution (which for $k = 2$ is indistinguishable from the true solution).

7. CALCULATIONS FOR A CONTROL SURFACE

Since there is no upstream influence in linearized transonic flow the theory given in Section 4 could be applied to the calculation of pressures

due to the motion of an arbitrarily shaped control surface on any planform with an unswept trailing edge and stream-wise side edges. Only a rectangular control surface will be treated here, however. For a full-span control surface the results of the previous section could be directly applied. The general case with a part-span control surface with no span-wise deformation may be obtained by suitable superposition of solutions having $\Phi_z(y, 0) = W(s)$ for $\sigma_1 \leqslant y \leqslant \sigma$ and $\Phi_z(y, 0) = 0$ for $\sigma \leqslant y < \sigma_1$ in the transformed plane, where $y = \sigma_1$ is the location of an inner side edge. It is convenient in the present case to set $x = 0$ at the leading edge of the control surface and the control-surface chord equal to unity.

From Eq. (10) we find that

$$\Phi^{(0)}(y, +0) = \frac{i}{2} W \int_{\sigma_1}^{\infty} H_0^{(2)}(K|y - \eta|)\, d\eta \tag{42}$$

or, upon inversion by use of Eq. (24)

$$\varphi^{(0)}(x, y, +0) = -\frac{1}{2\pi} \int_{\sigma_1}^{\infty} d\eta \int_0^x \frac{d\xi}{x - \xi} e^{-i\frac{k}{2}\left[x - \xi + \frac{(y-\eta)^2}{x-\xi}\right]} w(\xi)\, d\xi \tag{43}$$

The feasibility of choosing $\eta = \infty$ as the upper limit of integration will be apparent shortly.

For the calculation of $\Psi^{(1)}$ we will assume that $K|\sigma - \sigma_1|$ is so large that in Eqs. (12) and (13) $\Phi^{(0)}$ may be replaced by its asymptotic value which can be found by aid of the formula

$$\begin{aligned} \frac{i}{2} \int_0^R H_0^{(2)}(Ku)\, du &= \frac{i}{2} \int_0^{\infty} H_0^{(2)}(Ku)\, du - \frac{i}{2} \int_R^{\infty} H_0^{(2)}(Ku)\, du \\ &\approx \frac{i}{2K} - \frac{1 + i}{2K^{3/2}} \frac{e^{-iKR}}{\sqrt{\pi R}} \end{aligned} \tag{44}$$

Hence for large positive values of y

$$\Phi^{(0)} \approx \left[\frac{i}{K} - \frac{1 + i}{2K^{3/2}} \frac{e^{-iK\rho_1}}{\sqrt{\pi\rho_1}}\right] W \tag{45}$$

and for large negative values

$$\Phi^{(0)} \approx \frac{1 + i}{2K^{3/2}} \frac{e^{-iK\rho_1}}{\sqrt{\pi\rho_1}} \quad W \tag{46}$$

where $\rho_1 = |y - \sigma_1|$ denotes the distance from the point on the y-axis to $y = \sigma_1$. When introducing these into Eqs. (12) and (13) for $\Psi^{(1)}$ and $\bar{\Psi}^{(1)}$ it is seen that the same integrals are obtained as for $\Psi^{(1)}$ and $\Psi^{(2)}$ in the previous section (cf. Eqs. (32) and (38). Note, however, that the

expression for $\Phi^{(0)}$ in Eq. (46) differs from that of $\overline{\Psi}^{(1)}$, Eq. (38), in Section 6, by a factor of $2^{-\frac{1}{2}}$). Thus the previous results may be applied directly. When calculating $\overline{\Psi}^{(2)}$ we notice that the dominating term of $\Psi^{(1)}$ is the one originating from the first (strip-theory) term in the expression for $\Phi^{(0)}$, Eq. (45), so that, $\overline{\Psi}^{(2)}$ to the first order must be equal to $\overline{\Psi}^{(2)}$ of the previous section. Finally $\Psi^{(2)}$ may be neglected in comparison with $\overline{\Psi}^{(2)}$ so that the only solution required in addition to those of Section 6 is that for $\varphi^{(0)}$, Eq. (43).

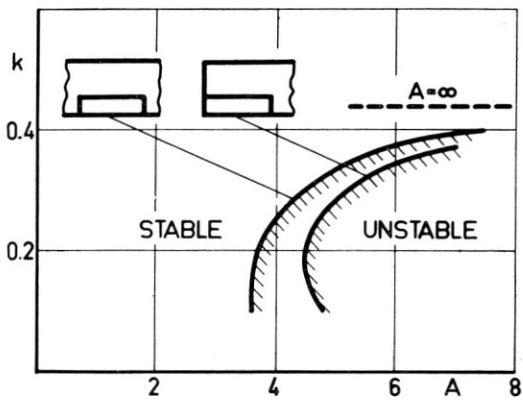

FIG. 8. Curves for zero hinge-moment damping at $M=1$ on rectangular control surfaces (hinge at the leading edge).

The theory is applied to the calculation of the hinge-moment-damping coefficient. This is given by $(1/k)L''_{22}$ (setting $x = 0$ at the hinge and assuming the aileron to have no aerodynamic balance). A positive L'_{22} indicates negative damping, i.e. a one-degree-of-freedom flutter of the aileron is possible. In Fig. 8 is calculated the stability boundary for the rectangular control surface, i.e. the values of A and k for which $L''_{22} = 0$. Two different locations for the control surface are considered, an outer one with one free side edge, and an inner one for which the control surface is assumed to be situated sufficiently far inboard so that the effect from the side edges of the planform on the control-surface pressure distribution may be neglected. It is seen that stability could always be achieved by a low enough aspect ratio and, of course, a high enough natural frequency of the control surface. Also the outer location is more favourable from a stability point of view than the inner one. The effect of the position of the control surface is further demonstrated in Fig. 9. The case considered is a rudder of $A = 4$ oscillating at $k = 0{\cdot}3$. The horizontal tail surface is assumed to act as an infinite reflecting plane. The two curves given are the span-wise distribution of $(1/k)L''_{22}$, i.e. $(1/k)l''_{22}$, on the rudder for the two different positions shown in the accompanying sketches. It is remarkable that moving the rudder upwards a distance of only one chord length so that the upper side edge becomes a free edge will remove the strong negative damping over most of the rudder and hence make it stable.

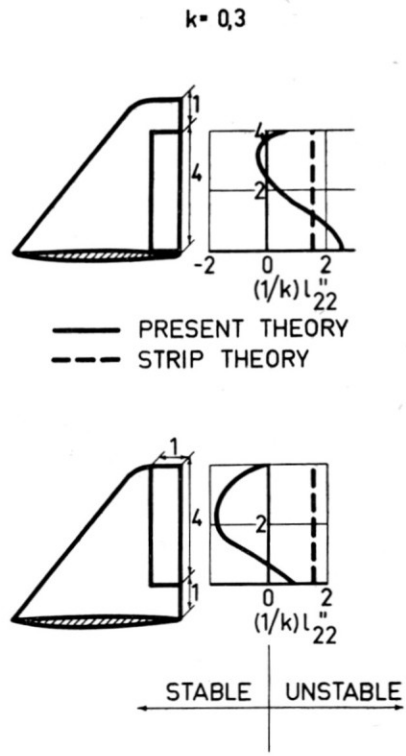

FIG. 9. Hinge-moment damping distribution on two $A = 4$ rudders at $M = 1$.

8. SOLUTION FOR DELTA WINGS

The principle of successive cancellation of lift outside the side edges employed above could possibly also be utilized for other wings with planforms composed of straight edge segments. Actually, by introducing oblique co-ordinates, it is possible to find the solution corresponding to Eq. (12) for any swept edge. The principal difficulty remains, however, to ascertain the convergence of the series corresponding to Eq. (22), in particular near corners formed by two subsonic edges.

For one particular planform, namely the triangular one, it is possible to obtain the exact solution in a different manner. In Eq. (2) (with $M = 1$) the following transformations are introduced

$$Y = y/x \qquad Z = z/x \qquad X = -1/x \tag{47}$$

$$\varphi = Xe^{i\frac{k}{2}\left[X + 1/X + (Y^2 + Z^2)/X\right]}\,\Omega(X, Y, Z) \tag{48}$$

By Eq. (47) the triangular wing is transformed to a pseudo-rectangular one with the leading edge at $X = -\infty$ and the trailing edge at $X = -1$ (see Fig. 10). The remarkable thing about the transformation Eq. (48) is

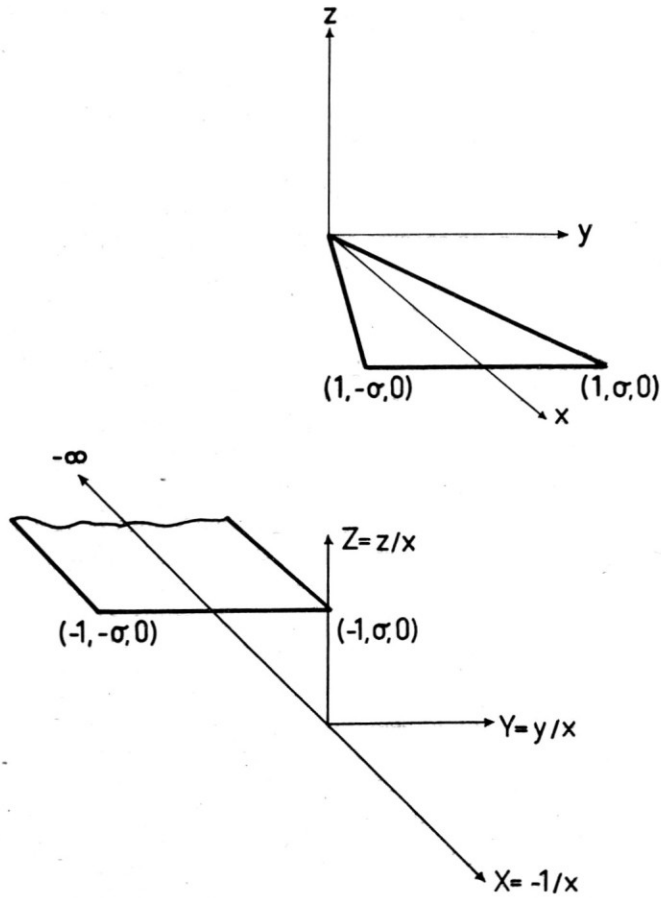

FIG. 10. Co-ordinate transformation for the delta wing.

that it will make Ω a solution of the transonic equation (2) in the new co-ordinate system. Thus

$$\Omega_{YY} + \Omega_{ZZ} - 2ik\Omega_X + k^2\Omega = 0 \tag{49}$$

Consequently the problem for the delta wing is reformulated to that for a rectangular wing with the tangency condition

$$\Omega_Z(X, Y, 0) = -\frac{1}{X^2} e^{-i\frac{k}{2}\left[X + 1/X + Y^2/X\right]} w(-1/X, -Y/X) \tag{50}$$

(for $-\infty \leqslant X \leqslant -1$, $|Y| \leqslant \sigma$).

The transformation thus makes it possible to solve the problem exactly by use of the rectangular-wing solution. However, for $X \to -\infty$, i.e. near the apex of the delta wing, the series, Eq. (22), given in Section 4 for the loading on the rectangular wing will not converge in general. The reason is

that, as is easily shown from the above equations, the correct loading should there approach that given by slender-wing theory (provided w is a smooth function of x near the apex) and this corresponds to $K\sigma = 0$ in Eq. (16) for which the series does not converge. The limitation is probably not serious from a practical point of view, however, since in most flutter cases one is interested in modes for which the wing apex does not move.

The presented transformation certainly opens up several interesting possibilities but, so far, no specific applications have been made.

9. CONCLUSIONS

The method presented in Section 4 allows the calculation, according to linearized theory, of generalized aerodynamic forces on any rigidly or flexibly oscillating rectangular wing provided the aspect ratio and reduced frequency are different from zero. Starting with the solution for a wing of infinite span, the solution was obtained as an infinite series which apparently converges rapidly even for fairly low values of $A\sqrt{k}$. Thus three terms in the series are sufficient in the case of a rigidly oscillating wing of $A = 2$ for $k \geqslant 0{\cdot}2$. This covers probably the complete range of validity of linearized theory. The numerical results confirm the conclusion reached in an earlier investigation[11] that three-dimensional effects are always very large, even for fairly large values of $A\sqrt{k}$.

From the calculations for a rectangular control surface one may conclude that the aerodynamic hinge moment damping is strongly affected by the geometry. Thus a control surface with an aspect ratio less than 3·5 is always damped regardless of its natural frequency. If the control surface has one outer, free, side edge it will have positive damping for $A < 4{\cdot}5$. However, the use of linearized theory for an oscillating control surface is questionable for two reasons: (1) The reduced frequencies of interest (based on control surface chord) are usually low so that the requirement (1) may not be fulfilled. (2) A shock wave may be located immediately ahead of the control surface causing "buzz", a non-linear phenomenon. A simplified method to treat this phenomenon in two-dimensional flow has very recently been suggested in Ref. 12.

In Section 8 a transformation was given which enables the exact solution for a delta wing to be found, provided the solution for a corresponding rectangular wing is known. However, no numerical applications have so far been made.

APPENDIX

Calculation of $h_0(x, y)$

The inversion of $\Psi^{(1)}(r)$ defined by Eq. (37), may be written

$$\psi^{(1)}(x, r, \pi) = \int_0^x h_0(x - \xi, r) e^{-i\frac{k}{2}(x-\xi)} w(\xi)\, d\xi \tag{A1}$$

where

$$h_0(x, r) = \mathscr{F}^{-1}\left\{H_0\left(s - \frac{k}{2}\right)\right\} \tag{A2}$$

and, according to Eq. (36),

$$\sqrt{2\pi} H_0(s) = \frac{i-1}{K}\left[F(Kr) - \frac{1}{2} + \frac{i}{2}\right] \tag{A3}$$

We must choose k to have a negative imaginary part, however small. Then the proper cut in the complex s-plane to make $(ks)^{\frac{1}{2}}$ occurring in Eq. (A2) single-valued is a straight line from the origin to infinity in the first quadrant making the angle $-\arg k$ with the real s-axis (see figure below). The inversion integral reads

$$h_0(x) = \frac{1}{\sqrt{2\pi}} \int_{-\infty}^{\infty} e^{isx} H_0(s - k/2)\, ds \tag{A4}$$

The path of integration should be taken below the branch-point for $(2ks)^{\frac{1}{2}}$, i.e. below the real axis. We complete the path of integration as shown in the figure below.

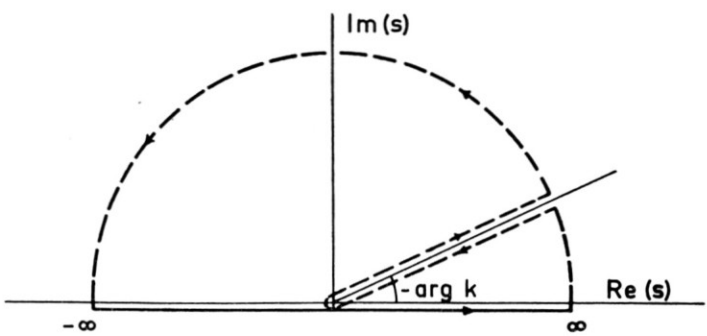

Since no poles are enclosed the integral along this path is zero. Also, for the branch $\mathrm{Im}\{(2ks)^{\frac{1}{2}}\} < 0$, $H_0(s - k/2)$ goes to zero along the semi-

circle at infinity so the contribution from this part is zero (Jordan's lemma). Hence

$$h_0(x) = \frac{1}{\sqrt{2\pi}} \int_L e^{isx} H_0(s - k/2)\, ds \tag{A5}$$

where L is shown below.

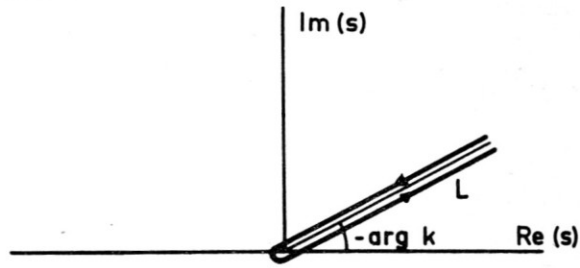

Along L, $H_0(s - k/2)$ may be expanded in the following series, convergent for all values of s, including $|s| = \infty$

$$H_0(s - k/2) = \frac{2^{\frac{1}{4}} e^{3\pi i/4}}{2\pi k^{\frac{1}{4}}} \sum_0^\infty \frac{(-i)^n (2k)^{n/2} r^{n+\frac{1}{2}} s^{n/2-\frac{1}{4}}}{n!\,(n+\frac{1}{2})} - \frac{i}{2(\pi k s)^{\frac{1}{2}}} \tag{A6}$$

Hence we may substitute Eq. (A6) in Eq. (A5) and integrate term by term. This leads to integrals of the type

$$\int_L e^{isx} s^{n/2-\frac{1}{4}}\, ds$$

These can be evaluated by means of the following formula for the definition of the gamma function

$$\int_L s^{-\alpha} e^{-s\delta}\, ds = \frac{2\pi i(-\delta)^{\alpha-1}}{\Gamma(\alpha)} - \tag{A7}$$

$$-\left(\frac{\pi}{2} - \arg k\right) < \arg \delta < \frac{\pi}{2} + \arg k$$

Then, setting $\delta = -ix$, and with $\arg k < 0$, the final result may be written

$$h_0 = \frac{1}{\sqrt{\pi k x}} \left[g_0(v) + \frac{1-i}{2} \right] \tag{A8}$$

where

$$g_0 = \sum_0^\infty \frac{e^{\frac{7\pi i}{8} - \frac{\pi i n}{4}} \cdot 2^{n/2-\frac{1}{4}} v^{\frac{1}{2}+n}}{n!\,(n+\frac{1}{2})\,\Gamma(\frac{1}{4} - n/2)} \tag{A9}$$

and

$$v = r\sqrt{\frac{k}{x}} \tag{A10}$$

REFERENCES

1. C. C. Lin, E. Reissner and H. S. Tsien, On Two-dimensional Non-steady Motion of a Slender Body in a Compressible Flow, *J. Math. Phys.*, Vol. 27, No. 3, October 1948.
2. J. W. Miles, Linearization of the Equations of Non-steady Flow in a Compressible Fluid, *J. Math. Phys.*, Vol. 33, No. 2, July 1954.
3. M. T. Landahl, E. L. Mollo-Christensen and H. Ashley, Parametric Studies of Viscous and Non-viscous Unsteady Flows, OSR Technical Report No. 55-13, 1955.
4. M. T. Landahl, Theoretical Studies of Unsteady Transonic Flow, Part I, Linearization of the Equations of Motion, Aer. Res. Inst. of Sweden (FFA), Report 77, 1958.
5. M. T. Landahl, Part II, The Oscillating Semi-infinite Rectangular Wing, Aer. Res. Inst. of Sweden (FFA), Report 78, 1958.
6. M. T. Landahl, Part III, The Oscillating Low-aspect-ratio Rectangular Wing, Aer. Res. Inst. of Sweden (FFA), Report 79, 1958.
7. J. W. Miles, On the Low Aspect Ratio Oscillating Rectangular Wing in Supersonic Flow, *Aero. Quart.*, Vol. 4, Part 3, pp. 231–44, August 1953.
8. K. Schwarzschild, Die Beugung und Polarization des Lichts durch einen Spalt. I. *Math. Ann.*, Vol. 55, pp. 177–247, 1901.
9. J. C. Gunn, Linearized Supersonic Airfoil Theory, *Phil. Trans. Roy. Soc.*, Vol. 240, pp. 327–373, 1947.
10. H. C. Nelson and J. H. Berman, Calculations on the Forces and Moments for an Oscillating Wing-aileron Combination in Two-dimensional Sonic Flow, NACA Report 1128, 1953.
11. M. T. Landahl, The Flow around Oscillating Low-aspect-ratio Wings and Wing-body Combinations at Transonic Speeds, Paper presented at the IXth International Congress of Applied Mechanics, Brussels, 1956.
12. G. Coupry and G. Piazzoli, Étude du flottement en régime transsonique. *La Recherche Aéronautique*, No. 63, mars–avril 1958.